

# Structural strength analysis of a rotary drum mower during harvesting

H. Kursat Celik,<sup>1</sup> Ibrahim Akinci,<sup>1</sup> Nuri Caglayan,<sup>2</sup> Allan E.W. Rennie<sup>3</sup>

<sup>1</sup>Department of Agricultural Machinery and Technology Engineering, Akdeniz University, Antalya, Turkey;

<sup>2</sup>Department of Mechatronics Engineering, Fac. of Engineering, Akdeniz University, Antalya, Turkey;

<sup>3</sup>School of Engineering, Lancaster University, United Kingdom

## Abstract

A rotary drum mower (RDM) is a tractor-mounted mechanism used for harvesting green fodder crops. It faces dynamic forces from rough field surfaces and cutting resistance, posing design challenges and potential failures. This study aims to present a well-designed procedure for analyzing the structural strength of an RDM during harvesting, employing both experimental and engineering simulation methods. A specific harvesting scenario was created to simulate realistic load conditions. Experimental testing and advanced computer-aided engineering (CAE) simulations

were conducted. Tractor power take-off torque measurements during harvesting revealed values of 231.07 Nm, 264.44 Nm, and 269.39 Nm at speeds of 8.56 km h<sup>-1</sup>, 12.6 km h<sup>-1</sup>, and 16.23 km h<sup>-1</sup>, respectively. Finite element analysis (FEA) was conducted to determine stress levels in the RDM components (RDM165-A-004, RDM165-B-003, and RDM165-B-004). The FEA stress results ranged from 5.070 MPa to 20.600 MPa, 13.800 MPa to 28.600 MPa, and 5.400 MPa to 27.550 MPa, respectively. Experimental testing yielded stress results ranging from 2.127 MPa to 18.600 MPa, 14.618 MPa to 33.229 MPa, and 8.838 MPa to 31.248 MPa, respectively. The comparison between experimental and FEA results showed a reasonable correlation. FEA visual outputs provided insights into the maximum equivalent stress and deformation distributions on the RDM, with no indications of failure in the machine's structure observed in either the experimental or numerical analyses. In conclusion, this study demonstrates that the machine analyzed operates safely under harvesting conditions. Moreover, the combination of experimental and advanced CAE methodologies presented in this research offers a valuable approach for future investigations into the complex stress and deformation evaluations of rotary drum mowers.

Correspondence: H. Kursat Celik, Department of Agricultural Machinery and Technology Eng., Akdeniz University, 07070, Antalya, Turkey.  
Tel.: +90.2423106570 - Fax: +90.2423102479.  
E-mail: hkcelik@akdeniz.edu.tr

Key words: rotary drum mower; agricultural machinery; strength analysis; experimental stress analysis; finite element analysis.

Contributions: HKC, project administration, investigation, visualization, formal analysis; HKC, NC, writing of original draft; NC, data curation; NC, IA, methodology; IA, conceptualization, resources; AEWR, supervision, writing, review and editing. All the authors approved the final version to be published.

Conflict of interest: the authors declare no potential conflict of interest.

Funding: none.

Acknowledgments: this paper is a part of Ph.D. research presented in the thesis of Dr. H. Kursat Celik, supported financially by The Scientific Research Projects Coordination Unit of Akdeniz University (Turkey) (Project No: 2011.03.0121.006).

Received: 30 June 2023

Accepted: 15 October 2023.

©Copyright: the Author(s), 2024

Licensee PAGEPress, Italy

Journal of Agricultural Engineering 2024; LV:1557

doi:10.4081/jae.2024.1557

This work is licensed under a Creative Commons Attribution-NonCommercial 4.0 International License (CC BY-NC 4.0).

Publisher's note: all claims expressed in this article are solely those of the authors and do not necessarily represent those of their affiliated organizations, or those of the publisher, the editors and the reviewers. Any product that may be evaluated in this article or claim that may be made by its manufacturer is not guaranteed or endorsed by the publisher.

## Introduction

Since people first began domesticating animals, forage crops have been used (Horrocks & Valentine, 2000). Fodder crops, which mainly consist of grasses but may also include alfalfa, field peas, clovers, and various other grasses, are planted for the purpose of producing hay, silage, or green animal feed. These crops are of significant importance compared to other agricultural crops, as they require similar amounts of input, care, and management (Day *et al.*, 2009; El-Baily, 2022). Harvesting fodder crops among other cultivation practices is an important agricultural task. Harvesting fodder crops can be fundamentally carried out in two stages. These are cutting (mowing) and picking up mown crops from windrows. Although the fodder harvesters are mostly driven by agricultural tractors (Martinez-Valencia *et al.*, 2021), they may be self-propelled or pull-behind. Each fodder harvest theoretically starts with cutting, regardless of the intended use. Farmers might accomplish this by using rotary mowers (vertical axis) or conventional cutter bar mowers. Rotary mowers employ rotating discs or drums, whereas cutter bar mowers use reciprocating knives to cut the plant. Vertical axis mowers avoid many of the issues that reciprocating machines experience by using freely pivoting blades attached to rotating shafts to cut the crop (Srivastava *et al.*, 2013). Vertical-axis rotary mowers can be divided into two types: disc and drum.

Tractor-mounted rotary drum mowers have a wide range of use in the harvesting of fodder crops with the advantages of adjustable cutting height, high quality of the cutting, durability, high ground speeds, *etc.*, most especially, for small- and medium-

sized agricultural enterprises. During the harvesting operation, the combination of the mowers revolution, forward velocity and plant cutting resistance cause the reaction forces that act on the machine elements and mowing mechanism and this may result in structural deformation which may cause undesired machine failure. Therefore, in the total design cycle of a rotary drum mower (RDM), it should be focused on two important perspectives: harvest mechanism and structural strength. In the design cycle of these types of machines, it is essential to determine the functioning and design limits of the machine components in accordance with the working conditions, and to establish and develop their design specifications within the design requirements and limits. The functioning and performance of machines are directly impacted by the structural design and durability of these systems or components. In order to prevent machine failures and maintain appropriate material weight and cost, structural durability assessment is one of the final steps before an agricultural machine prototype is released to the market (Paraforos *et al.*, 2016). For designers, manufacturers, service providers, and end users, durability has evolved into a valuable design element. Additionally, durability facilitates the employment of circularity solutions for extending product lifespan, such as reuse, repair, refurbishment, and remanufacture. A machine with improved functioning and material savings as a consequence of such a durable design is also essential for manufacturers (Mesa *et al.*, 2022). Unparalleled changes have been seen in computers' capacities to collect data, analyze, alter, and store it, as well as to disseminate and share information and use these abilities in a variety of contexts. In this regard, modern computer-aided design and engineering (CAD and CAE) technologies have taken on a major position for use in the machinery industry in recent decades, particularly within the arena of competitive product design activities. These applications serve to reduce effective operating cycles between traditional design processes and improve overall process efficiency (Bi, 2021; Chakrabarty, 2022; Rembold *et al.*, 1993). However, despite the expanding trend in CAE-based durability assessment, its development, application, and possible advantages might be gained from its usage in the product design

stage are not precisely traced by small- and middle-scale agricultural machinery manufacturers; most especially in Turkey, within the frame of implementation such new technological developments (Eryürük *et al.*, 2019).

In this paper, the focus is on the strength analysis of the structural components of the RDM. Previous research has examined the structural design of harvest mechanism's components (Celik & Akinci, 2015; 2016). However, limited information can be found in published literature regarding the strength-based design analysis of the structural components of a tractor-mounted RDM specifically during harvesting operations. To address this gap, this study presents a systematic approach to strength-based design analysis and conducts stress analyses using both experimental and advanced engineering simulation methods. The analyses were performed on a sample tractor-mounted RDM during harvesting, and all the necessary analysis steps were thoroughly executed. The study follows a structured sequence, including the introduction of the RDM, the work-cycle scenario, the experimental field test procedures, the FEA setup procedures, the FEA and field test results, the evaluation of the results, and the conclusion.

## Materials and Methods

### Rotary drum mower

The RDM studied in this paper was manufactured in Turkey by a local agricultural machinery manufacturing company. The company retains intellectual property rights via patent protection specific to this machine (Yuksel Tarim Inc., 2013). In the design of this machine, a belt-pulley system was disregarded, instead, a gearbox was utilized to transmit the movement from the tractor power take-off (PTO) to the drums (mowing mechanism). Additionally, this machine was designed as a tractor-mounted type and adjustment of the transport (road) and harvesting positions can be provided by a cylindrical piston unit controlled by the tractor-hydraulic system. Figure 1 provides the fundamental technical specifications of the RDM utilized in this study.

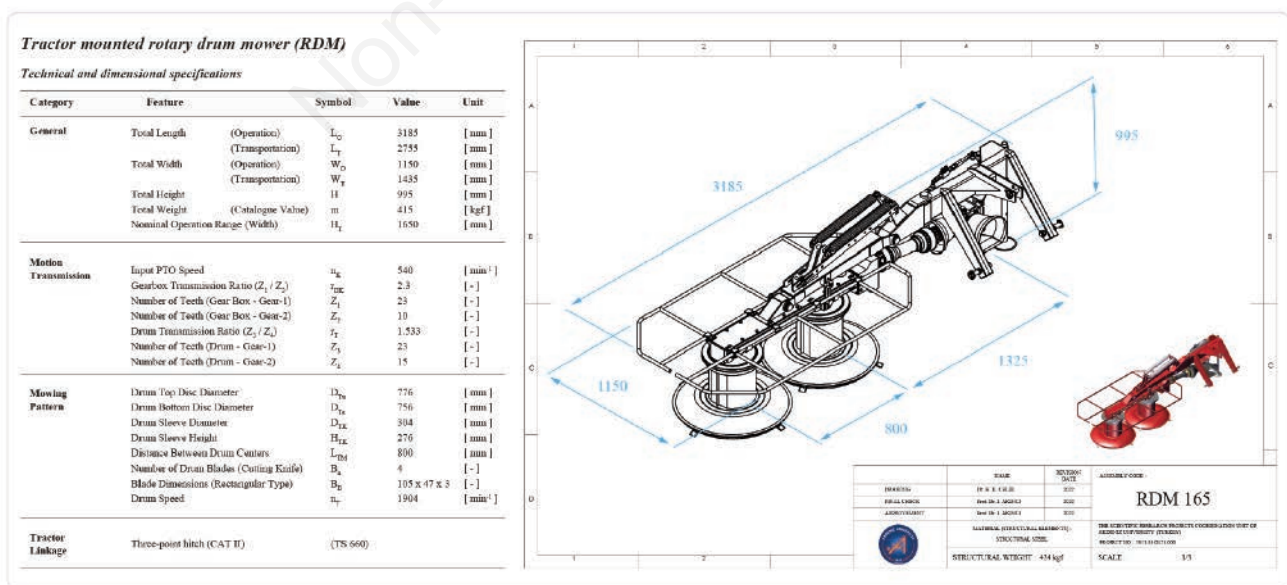


Figure 1. Technical specifications of the rotary drum mower.

## Work-cycle Scenario for the rotary drum mower

A successful design process for a machine system aims at providing intended functionality and durability within the specified design limits in the prescribed operation. From a durability perspective, the machine is assessed throughout by a strength-based design analysis process and it is expected that this will enable failure-free operation during the peak physical loading conditions. In the scope of the design assessment for the mower utilized in this paper, in order to adhere to design demands, the total work cycle of the machine including stationary position, transportation and harvesting operation should be clearly described. In this regard, a total work cycle scenario describing the RDM's operational circumstances was framed in this study. In this scenario, the machine's physical load conditions were assessed for three loading features: i) in-garage static linkage position; i) during transportation; iii) during harvesting operation. This paper covers the structural strength analysis of the machine during harvesting operations. In-garage static linkage position and during transportation on the way to the agricultural field were considered in another study (that has not been published yet), which is not in the scope of this paper. The framed total work cycle scenario for the RDM is illustrated schematically in Figure 2.

## Experimental set-up

### Confirmation of the material properties

Tensile tests were conducted to verify the material properties and determine the experimental failure threshold of the components related to the RDM. The manufacturing company confirmed that the structural components of the machine were made from standard machine-manufacturing steel materials. In both experimental and simulation-based stress analyses, the yield stress point of the material was designated as the failure threshold, using the von Mises failure criterion. The specimens used in the tests were obtained from the manufacturer's stocks, specifically from the components designated for RDM production. Nine type-2 rectangular specimens (resembling dog bones) with thicknesses of 2.5 mm, 6 mm, and 8 mm were employed, following the "TS EN ISO

6892 1" Metallic Materials Tensile Test Standard. The tests were conducted using a SHIMADZU AG-X 100 kN tensile capacity test device. The tensile test results confirmed that the average yield, ultimate tensile, and fracture strengths of the material were 280.26 MPa, 404.23 MPa, and 348.69 MPa, respectively (Figure 3). These results confirm the suitability of the steel-based materials used in the production of the RDM in terms of their manufacturing (structural) steel properties.

### Experimental strain measurement set-up

In order to assess the RDM's deformation behavior under in-field operating conditions and to evaluate the FEA outputs, experimental strain measurements were carried out on the machine during harvesting. Stress analysis for the targeted component groups was performed through strain data that were converted to equivalent stress values. The HBM K-RY81-6 series  $0^{\circ}/45^{\circ}/90^{\circ}$  three-element, 120 ohm rectangular rosette Strain-Gauges (SG) were used to measure the strain using a universal data acquisition module of HBM-QuantumX MX840A with eight channels and 24-bit resolution capability (HBM, 2011a; 2011b). Strain data were recorded at a sample rate of 50 Hz and simultaneously converted to equivalent stress values in the CATMAN data monitoring and processing software (HBM Inc., 2022). When selecting the SG bonding locations, consideration was given to the machine's essential loading locations, optimizable parts, and ability to represent high and low-stress distributions that could possibly affect the components under actual loading conditions. In the SG bonding procedures, the dimensional sizes of the components were also kept under consideration. Three SG rosettes were employed for the component RDM165-A-004 and seven SG rosettes for the components RDM165-B-003 and RDM165-B-004. SG bonding surfaces on the components were mechanically prepared, cleaned by using a chemical solvent (M-Bond 200 Catalyst) and bonding was realized through Vishay M-Bond 200 SG adhesive (Hoffmann, 1989; Vishay, 2007). Finally, to protect the SG surfaces from the damaging effects of the environment, a special coating tape and cold silicone are utilized. Details related to SG bonding applications on the specified components are shown in Figure 4.

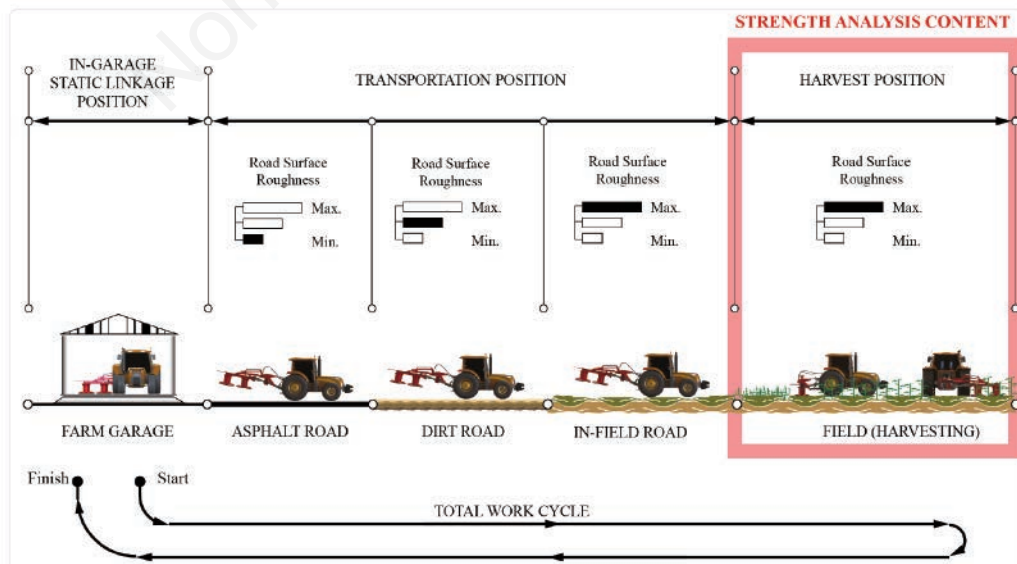


Figure 2. Total work cycle scenario for rotary drum mower.



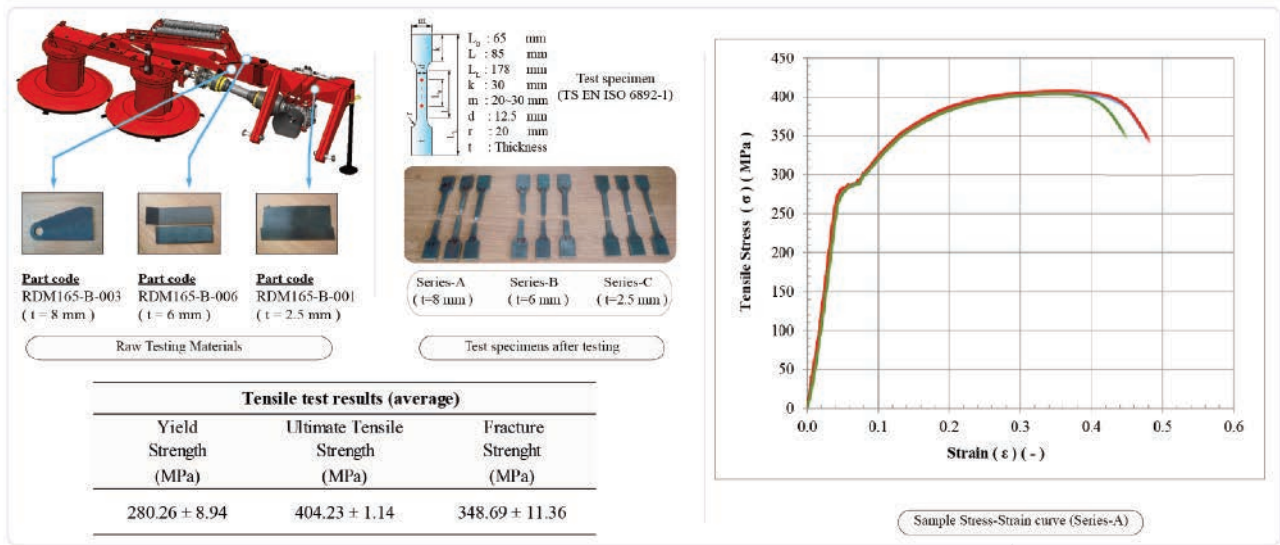


Figure 3. Material confirmation tensile tests.

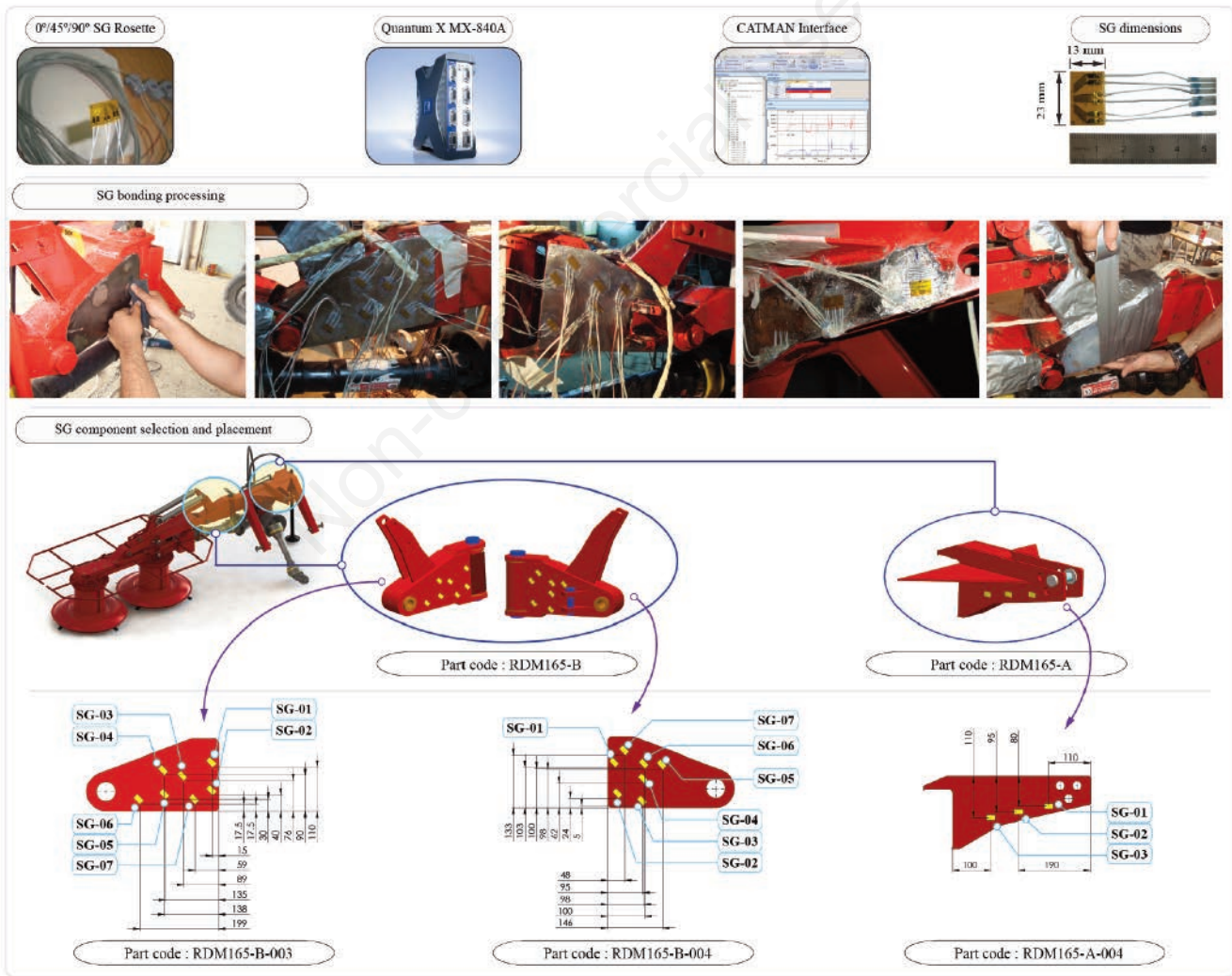


Figure 4. Details of the Strain-Gauges application.

### Field tests

Field tests were carried out by harvesting alfalfa (*Medicago L. species*) in a 150×350 m (52.5 da) field belonging to a local agricultural enterprise in Kadriye town, Serik district, Antalya province in Turkey. During the harvesting process, it is important to take into account the agricultural properties of the plants to be harvested in terms of determining the mowing parameters. It is likely that there will be differences in shear resistance values among forage crops such as alfalfa, sainfoin, vetch *etc.* (Turker, 1992). However, in the literature, no data were found showing that these differences have a significant effect on the loading conditions that the RDM is exposed to during the harvesting process.

It is recommended to harvest alfalfa between the time 10% of the plants start to bloom and the time when the flowering reaches 33% of the plants (TRMoNE, 2012). All tests were carried out at the appropriate harvest time, taking into account the given flowering rates of the alfalfa plant. Measurements of the relevant agricultural data were carried out with reference to 'Measurement of the Agricultural Data - Technical Instruction for Alfalfa Plant Species' published by Turkish Republic, Ministry of Food, Agriculture and Livestock (TRMoFAL, 2001). At the measurement locations determined on the harvest area, a 500x500 mm frame was used and the plants within this frame were collected, and some physical dimensions of the plants were measured using a tape measure and digital calliper on randomly selected samples from each measurement location (25 specimens for each). The plant specimens taken from the field were transported to the laboratory retaining their moisture content. NUVE-FN 120 Model, +5-250°C working temperature and 120 L volume capacity drying oven was utilized and the specimens were tested at 70°C for 48 hours. A precision scale (A&D-GF-600) with an accuracy of 0.001 g was used to measure the fresh and dry weights of the specimens. The moisture content of the specimens was determined according to the wet base.

In the field tests, the harvest position of the machine was set up and the worst working conditions were considered during the mowing process. There is a spring system on the functional element group of the machine. Thus, the functional element group can move against the surface roughness in the direction of gravity on the soil surface. During the tests, the machine is mainly loaded with a draft force in the opposite direction of the tractor's progress rather than the effect of gravity. In this case, the physical deformation evaluation of the machine was carried out by evaluating the equivalent stress values obtained by processing the strain measurement data taken on the previously selected components. A New Holland-TD75D Model, 2WD-75 HP agricultural tractor was utilized in the field tests. All field tests were carried out at 540 min<sup>-1</sup> tractor PTO speed, with three repetitions, at three different tractor speeds. The signal flags were placed at 40 m intervals in the direction of the tractor's progress, and the time that the tractor took to cover the distance between the two signal flags during the tests was measured with a digital stopwatch and the tractor progress rate was calculated separately for each repetition using Equation 1.

$$V_t = \frac{X}{t} \quad (1)$$

Here,  $V_t$  is the tractor's forward speed (ms<sup>-1</sup>),  $X$  is the distance between two flags (m), and  $t$  is the travel time (s).

In the field tests, the torque measurement values of the tractor PTO were recorded separately for each repetition using a computer-aided measurement system at three different tractor speeds by placing a torque meter between the PTO and the universal shaft that

mediates the first motion transmission to the machine. Additionally, the measurement of the torque value required by the machine to rotate the drum group to be used in the relevant evaluations was carried out in the garage environment by operating the machine in the harvesting position. DATUM-Electronics, 420 Series, 0-1800 Nm capacity computer-aided measuring system and DATUM-Torque log software were used to measure and record torque data. In all measurements, the machine was operated with 540 min<sup>-1</sup> PTO speed and the sample rate during data recording was 10 Hz. As a power machine, the transmission of the movement from the tractor to the work machines in the form of draft power is provided with a three-point hitch or drawbar. During traction power transmission, there are some losses depending on parameters such as power losses in the motion transmission organs, ground properties, rolling resistance, skidding, *etc.* As a result, there is a partial transmission of tractor engine power to draft power (Sabanci & Akinci, 2012). ASAE Standard D497.7 describes the correlation between tractor PTO power and draft power (ASAE D497.7 - Agricultural Machinery Management Data, 2011). As such, tractor draft force was calculated from the experimental tractor PTO power data measured during the harvesting operation in the field tests using Equations 2 and 3 (Theunissen, 2002; Walters, 2021).

$$P_{PTO} = \frac{T_{PTO} \cdot n_{PTO}}{9550} \quad (2)$$

$$P_{PTO}(0.72) = P_{Draft} = F_{Draft} V_{Tractor} \quad (3)$$

where  $P_{PTO}$  is PTO power (kW),  $P_{Draft}$  is draft power (kW),  $n_{PTO}$  is PTO speed (min<sup>-1</sup>),  $T_{PTO}$  is PTO torque (Nm),  $V_{Tractor}$  is tractor speed (m s<sup>-1</sup>) and  $F_{Draft}$  is draft force (kN).

Accordingly, the average values of some agricultural data obtained in the measurements of the alfalfa plant, tractor speeds, PTO torque measurements, schematic descriptions of the physical loading of the RDM and related pictures taken during harvesting in the field tests are given in Figure 5.

### Finite element analysis

The FEA study was carried out for the RDM in the harvesting position in order to exhibit the deformation behavior of the machine during harvesting and to compare numerical and experimental analysis results. Specific to finite element method, related analysis steps were followed.

Since the manufacturer did not have a comprehensive CAD model that could be used for the FEA, a reverse engineering approach was employed to handle the solid modeling procedures for the RDM. In this procedure, each component of the machine was disassembled, measured and digitized through SolidWorks 3D parametric solid modeling software. The RDM's real-world mobility was reflected in the CAD model assembly. Almost all of the parts of the machine were made of steel-based materials. In motion transmission components, rubber-based polymers were used for bedding and sealing. Material properties of these components were assigned in the CAD model (Table 1).

One of the criteria taken into account while deciding whether the CAD models created can effectively represent real-world structures is the mass criterion. In order to validate the mass criteria of





**Figure 5.** Agricultural data of the alfalfa plant and physical loading test of the rotary drum mower.

**Table 1.** Material properties assigned in the computer-aided design modeling and the finite element analysis study.

Properties*	Unit	Components			
		Structural steel	Spring (DIN EN 10270-1)	Key/Pin/Shaft (DIN 1.5755 / 31NiCr14 / AISI 3330)	Bolt-Nut standard: 8.8
Modulus of elasticity	(GPa)	210	210	210	210
Poisson's ratio	(-)	0.3	0.28	0.3	0.3
Yield strength (max.)	(MPa)	280**	700	550	640
Ultimate tensile strength (max.)	(MPa)	404**	1000	750	800
Density	(kg m <sup>-3</sup> )	7850	7850	7850	7850

\*Finite element analysis definition: homogeneous isotropic linear elastic material model; \*\*experimental. **DIN**; **EN**; AISI, American Iron and Steel Institute.

the solid model, physical weight measurements were realized on the structural and functional groups of the machine. A computer-aided measurement system and a ZEMIC H3-C3-5.0t-B6 model 50 kN capacity S-type load cell were utilized to measure the machine weight. The weight measurements were recorded in the computer environment for 30 seconds at a sampling rate of 10 Hz with three repetitions. The solid modeling software calculated the RDM CAD assembly's overall mass to be 424.15 kg (experimental mass measurement value: 423.93 kg).

The CAD assembly has a large number of parts, so a simplification process was carried out without degrading the model's ability to structurally represent the physical machine. In this procedure, the structural components' initial geometries, the machine's total weight and the location of its center of gravity were preserved. The drum set and gearbox were reconfigured in the CAD model using rectangular prism geometry while retaining their original mass. Thus, the ideal solubility level for the FEA was provided by means of a re-configured CAD model. The physical measurement, solid modeling procedure, final assembly, re-configuration process and assembly statistics for the RDM CAD model are given in Figure 6.

The RDM is produced using both structural components and standard machine parts, such as steel plates, springs, bolts, nuts, pins, shafts, *etc.* The material properties of these components as assigned in the FEA were gathered from the literature provided by the applicable standards and existing material testing results of the machine's structural components. The material properties of the components used in the CAD modeling and the FEA solution are provided in Table 1. (Bringas, 2016; Cardarelli, 2008; Davis, 1998; Kulaksiz, 1995; Kutay, 2003; MKE, 1978; Rice *et al.*, 2003).

The boundary condition for the RDM in the FEA study was described with reference to the position where the machine was linked to the tractor and set up to the harvesting position. The draft force values as assigned in the FEA study were calculated through Equations 2 and 3 for each tractor speed and PTO torque values measured experimentally. Additionally, the gravitational constant was considered to be  $9.81 \text{ ms}^{-2}$ . Some of the RDM's components were welded together during production, while others were fastened together using detachable fasteners like bolt nuts and connecting pins. Therefore, bonded and frictionless contact definitions were given for associated components in the FEA setup.

The meshing functions of the FEA software were employed to construct FE models for the RDM. Mechanical-standard meshing approaches were applied in the meshing processes. Pre-trials on the FE model were conducted. As a result, the FE model was verified through a skewness metric that can measure whether the FE model accurately represents the actual model geometry. The definition of skewness states that a value of 0 denotes an equilateral cell (the best) and a value of 1 denotes a cell that has fully degenerated (the worst) (ANSYS Product Doc., 2019). For the FE model, the average skewness metric value found was 0.25, indicating excellent cell quality. After the completion of the pre-FEA steps, solution processes were performed and the results were recorded. The mechanical module of the ANSYS workbench multi-physics engineering analysis software was utilized in the strength analysis procedure. All analyses were conducted with the assumptions of homogenous isotropic linear elastic material model and linear static loading. The analysis-solving platform was a Dell Precision M4800 series mobile workstation (Intel Core i7-4910Q-2.9 GHz, 32 GB RAM, NVIDIA Quadro K2100M-2 GB, DDR5).

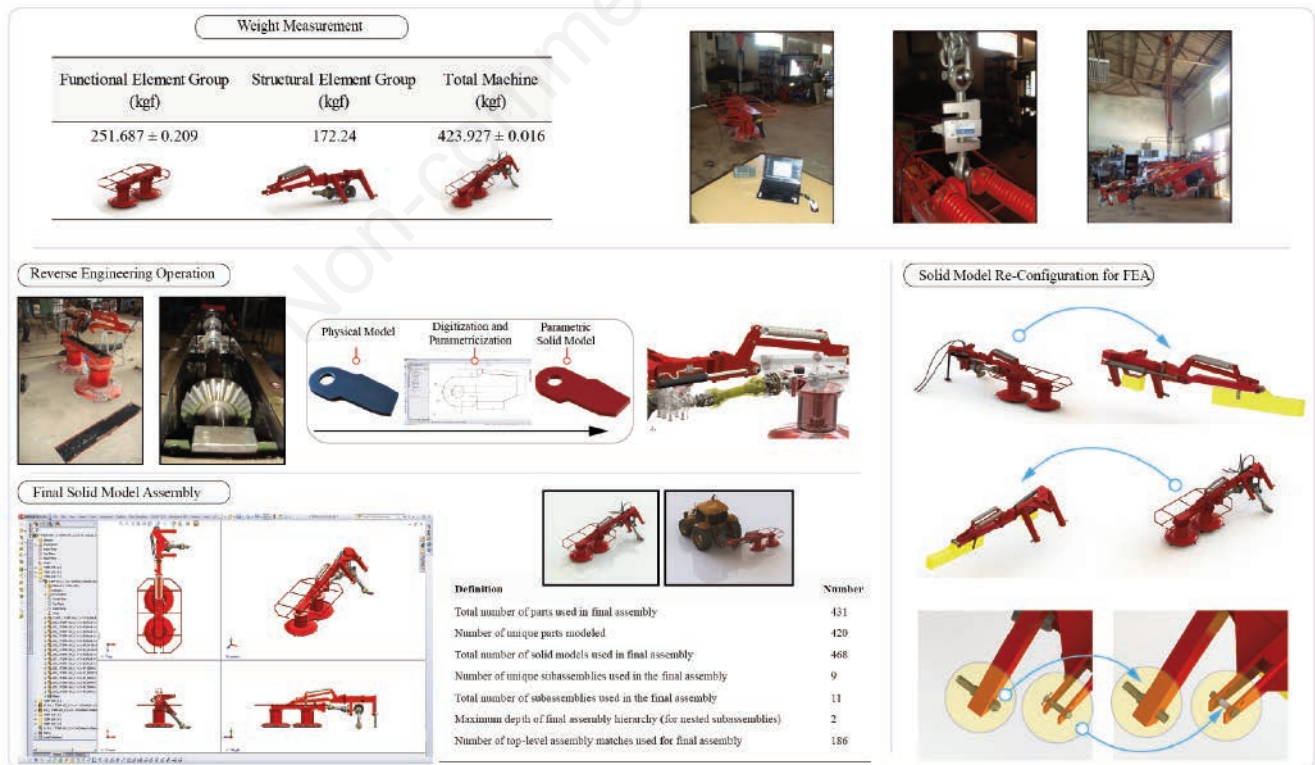


**Figure 6.** The physical measurements, solid modeling procedure, re-configuration for the finite element analysis and assembly statistics for rotary drum mower.



Description of the boundary conditions, maximum draft force calculations and the FE model details are illustrated in Figure 7.

## Results and Discussion

### Field test results

All of the data gathered from the physical testing was analyzed in order to assess how the machine would behave in terms of deformation under real-world harvesting conditions. Accordingly, tractor speed and PTO torque values that have been measured as well as the results of stress values that have been calculated on related components were analyzed. It was found from the literature on alfalfa crop harvesting with similar drum mowers that the harvesting process was carried out with a tractor forward speed of 8.5 km h<sup>-1</sup>, however, it was also found that the forward speed of this type of machine can be 10-12 km h<sup>-1</sup> depending on the working conditions (Arac, 2001). In the catalogue values for the RDM used in the physical tests within the scope of this research, it is stated that the tractor forward speed can be 15 km h<sup>-1</sup> depending on the suitability of the working conditions (for processes such as meadow harvesting on smooth land) (Yuksel Tarim Inc., 2013). In this regard, the tractor speed-01 (8.56 km h<sup>-1</sup>) and tractor speed-02 (12.86 km h<sup>-1</sup>) were determined during the harvest in physical tests and were compatible with the literature, and tractor speed-03 (16.23 km h<sup>-1</sup>) was higher than the literature and machine catalogue values. As a result, it was seen that the speed measured in the RDM physical tests was in a range that would force the machine under normal operating conditions and above normal operating conditions in accordance with the research purpose. Tractor PTO torque measurements in the field tests showed that the machine was loaded

with different torque values at different speeds during the mowing process (Figure 5). The test results revealed that PTO torque values increase with the increase of tractor speed during harvesting. Maximum PTO torque was measured as 269.39 Nm at a tractor speed of 16.23 km h<sup>-1</sup> (tractor speed-03). However, draft force calculations through PTO torque indicated that the maximum draft force of 3956.35 N was calculated at the lowest tractor speed of 8.56 km h<sup>-1</sup> (tractor speed-01). Considering the maximum torque values obtained from the physical tests as the values that put the most strain on the RDM motion transmission elements, the machine was loaded with a torque increase of approximately 2.95 times at the speed-01, 3.37 times at the speed-02, and 3.44 times at the speed-03 compared to the unloaded position. Therefore, it can be stated that the relevant values obtained under pre-defined operating conditions were the maximum loading conditions that guide the design limits of the structural and motion transmission elements of the machine for the harvesting operation.

The stress values obtained from the experimental stress analyses indicated that no value exceeded the material failure criterion (the yield strength of 280 MPa). The most challenging situations for the machine in terms of structure are the situations where the stress values reach the highest values. Machine design and structural optimization studies are carried out considering the situations where the relevant structure is under the highest load. For this reason, although the machine was exposed to excessive loads during the harvesting operation, particularly during the tractor speed-03 tests in the field, the other scenarios which are linked in garage and transportation positions described in the total work-cycle scenario must be analyzed. Subsequently, the decision-making process on related design parameters should be realized.

Consequently, for the harvesting scenario, it can be said that the relevant experimental data obtained during operating condi-

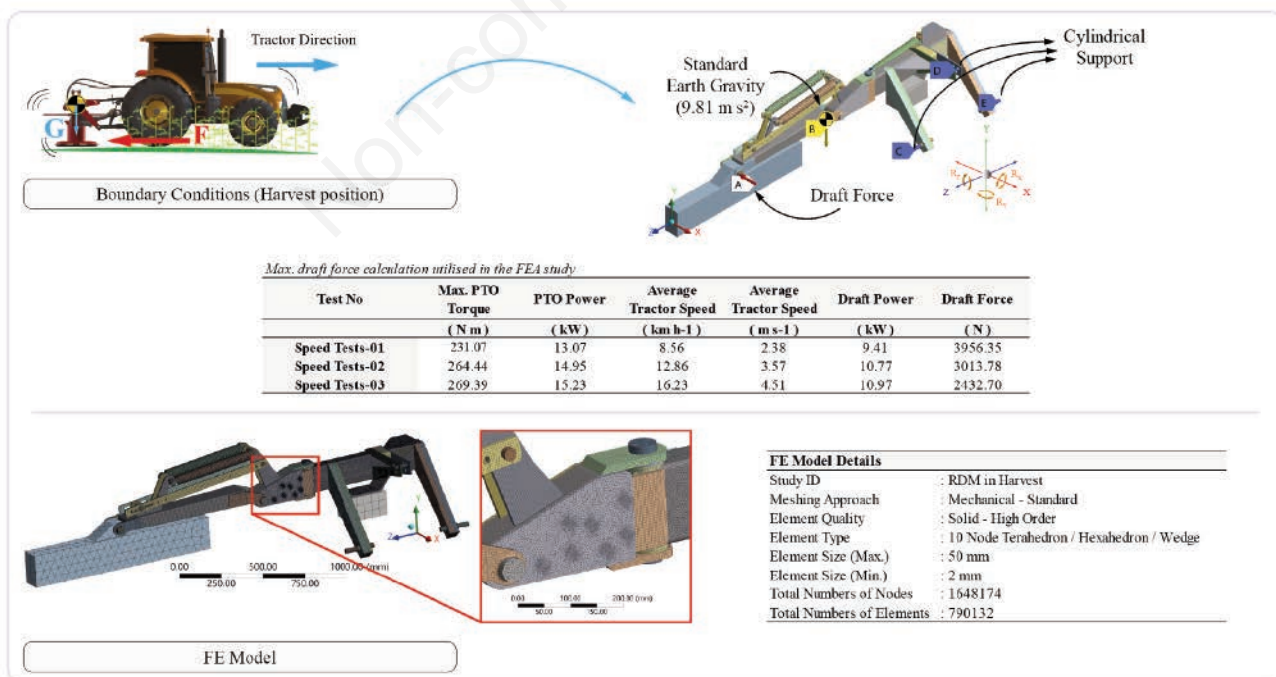


Figure 7. Boundary conditions and the finite element model details.



tions to be considered in the structural strength-based design of the RDM during harvesting and the field tests did not reveal any abnormal deformation behavior or permanent damage on the machine components during and after harvesting operation from a visual observation.

### Finite element analysis results

Numerical and visual outputs that exhibit the deformation behavior of the RDM during harvesting were obtained from the

FEA results. The results for the whole machine revealed that the maximum deformation (displacement) values were 18.377 mm, 14.778 mm and 12.598 mm against the tractor speed-01, tractor speed-02 and tractor speed-03, respectively. The maximum displacement location under the pre-defined boundary condition was around the connecting shaft of the drum group for all analyses. It can be stated that these values were very low relative to the overall machine size and would not exhibit any durability issues during harvesting.

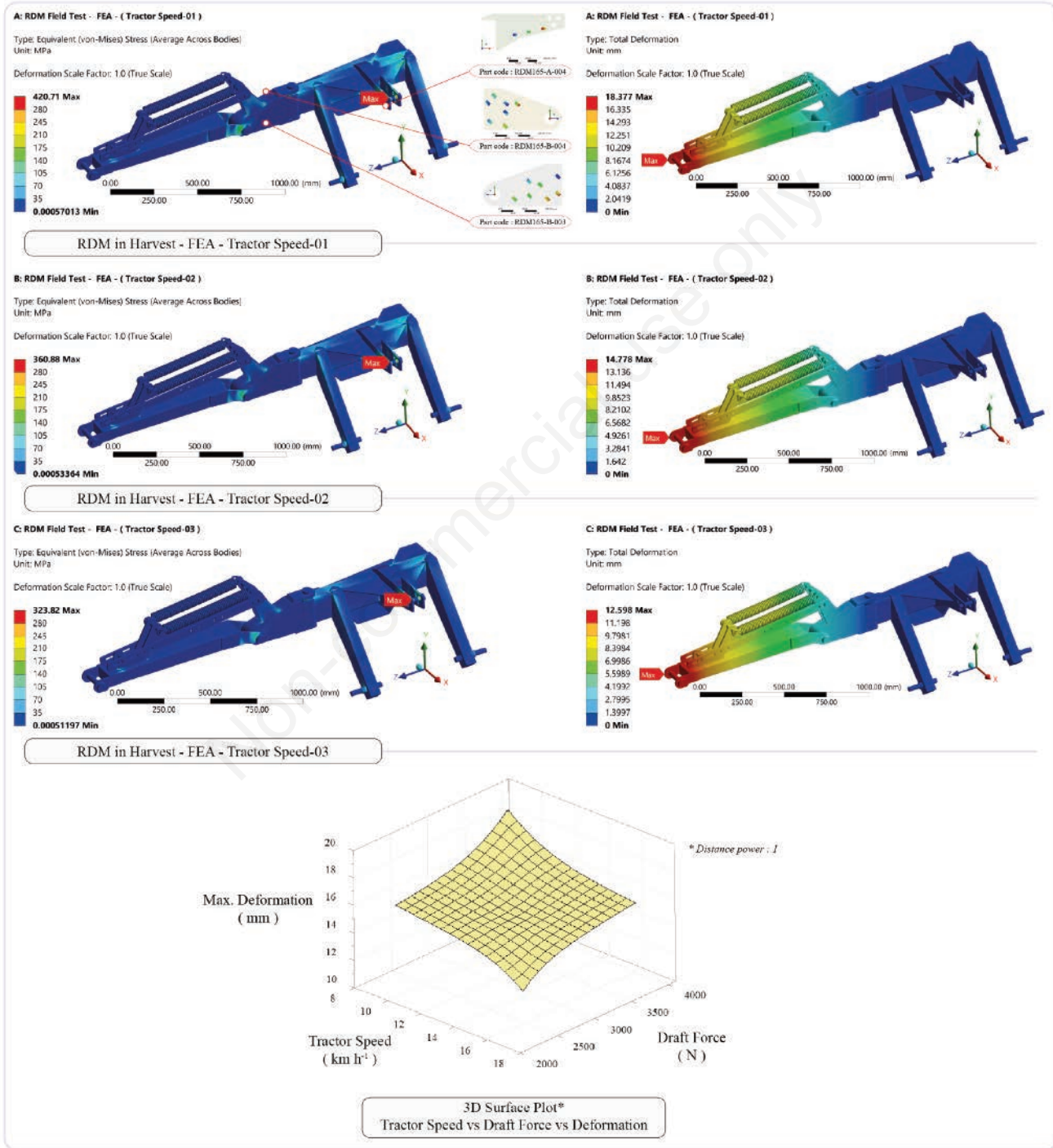
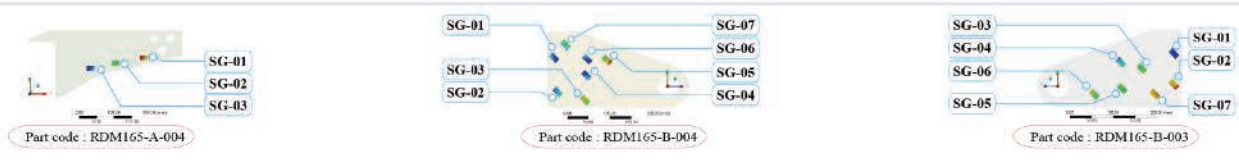
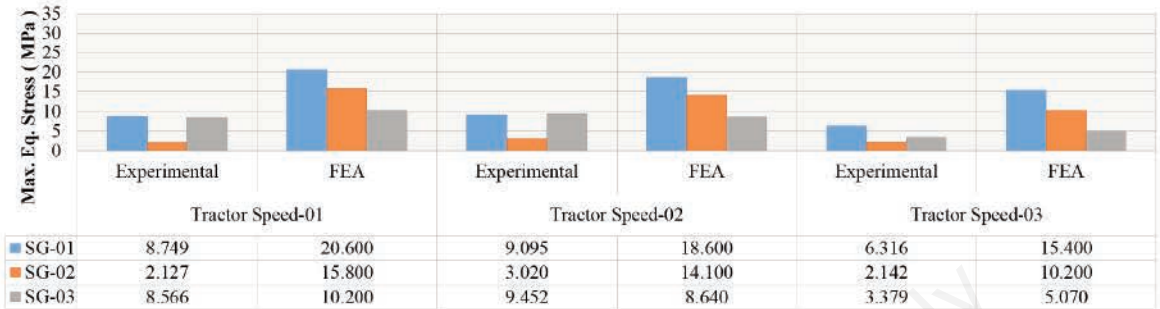


Figure 8. Finite element analysis visual outputs and 3D surface plot for deformation.

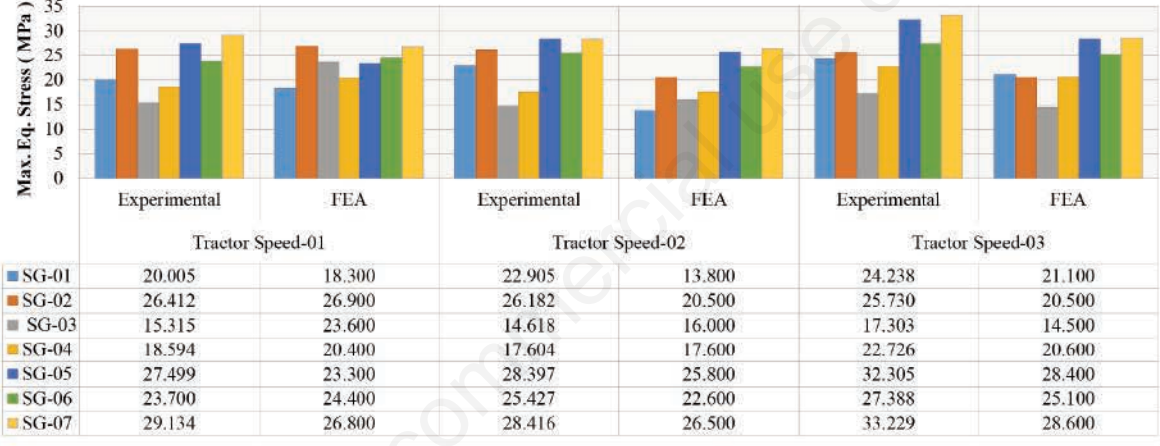


Equivalent stress values calculated on the SG bonding surfaces

**Part Code:  
RDM165-A-004**



**Part Code:  
RDM165-B-003**



**Part Code:  
RDM165-B-004**

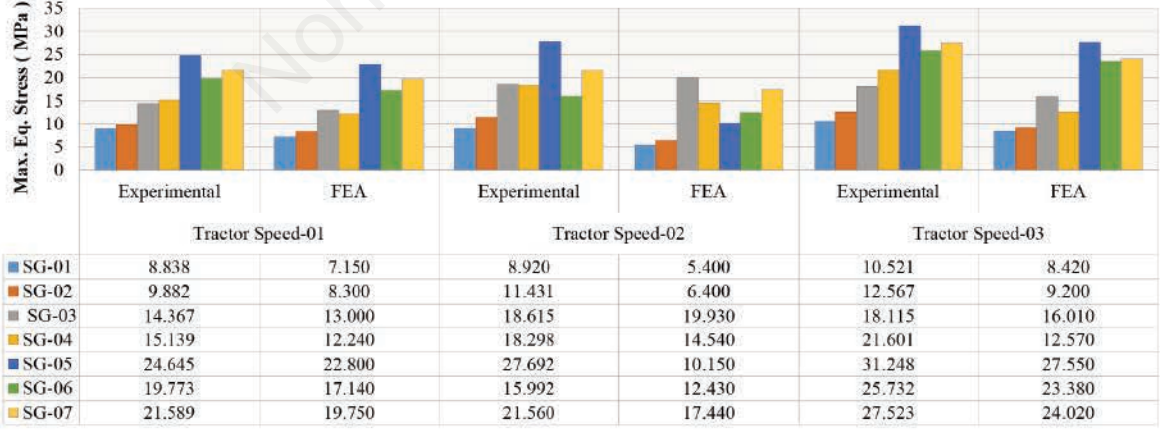


Figure 9. Numerical comparisons of experimental and finite element analysis results by the components.

The maximum equivalent stress values were 420.71 MPa, 360.88 MPa and 323.82 MPa on the upper hitch pins for tractor speed-01, tractor speed-02 and tractor speed-03, respectively. These stress values were below the hitch pin's failure point which is 550 MPa. No stress values that exceeded the failure threshold were determined on the other structural components of the RDM. The deformation and stress values highlighted that there was a decrease against an increase of the tractor speed in the harvesting scenarios. It can be said that the reason for the decrease in these values is that the velocity in the calculations of converting the PTO power to the drawbar (draft) power is proportionally high and the draft force values decrease against the increase in the velocity.

Additionally, numerical stress values taken from each SG location on the related components (RDM165-A-004, RDM165-B-003 and RDM165-B-004) in the FEA results were listed. On these components, it was noted that the corresponding stress distribution values were far below the material's failure threshold. These values were understood not to be a factor in the component groups' failure risk. The FEA visual outputs that illustrate the maximum equivalent stress and deformation distribution on the RDM and the 3D surface plot which exhibited the relation between tractor speed, draft force and deformation are given in Figure 8.

### Comparison between experimental and finite element analysis equivalent stress values

Experimental results are the key component of assessing the simulation outputs, hence, the comparison of the FEA results was made through related experimental stress results obtained on the specified components. The comparison result is given through a graphical representation in Figure 9. In most FEA studies, the calculated relative difference ratios were used to evaluate the simulation result against experimental results (Kurowski and Szabo, 1997). Studies with FEA validation that were given in a variety of scientific domains show that there are differences in the relative difference ratios that can be found when comparing experimental/theoretical analyses with FEA results. Although some literature claims that a well-established FEA approach should have a relative difference ratio of no more than 10% (Krutz *et al.*, 1984; Kuna, 2013), some studies show that different relative difference ratios can be found more than 10% depending on the analyses content, size and the assumptions when comparing the findings of FEA and experimental/theoretical analysis (Ariza *et al.*, 2015; Caliskan, 2011; Celik *et al.*, 2012; 2017; 2020; Degirmencioglu, 2003; Ruiz de Galarreta *et al.*, 2020; Torre & Brischetto, 2022; Yurdem *et al.*, 2019).

In this study, a relative difference ratio comparison was not utilized as the absolute values obtained from the experimental and FEA results were quite small. These small absolute values would provide a high percentage comparison which may not lead the designers to make an on-target evaluation for the analysis output. Therefore, absolute values of experimental and FEA results were compared and given in the format of a comparative chart (Figure 9). Accordingly, the absolute numerical values of experimental and FEA results were reasonably close to each other for the related components. Experimental stress results ranged between 2.127-18.600 MPa, 14.618-33.229 MPa and 8.838-31.248 MPa for the components coded RDM165-A-004, RDM165-B-003, and RDM165-B-004, respectively, while FEA stress results ranged between 5.070-20.600 MPa, 13.800-28.600 MPa and 5.400-27.550 MPa for the components coded RDM165-A-004, RDM165-B-003, and RDM165-B-004, respectively. The maximum absolute difference in numbers is approximately 22 MPa for

both experimental and FEA results on the SG bonding surfaces.

In a FEA study, limitations and errors based on numerical approach and user perspective are inevitable, such as limitations of modeling actual working conditions because of unexpected and unpredictable dynamic circumstances in the actual operating environments of the machine, FEA-specific problem-solving techniques, necessary presumptions that must be taken into account in order to deal with the constraints in the context of this numerical technique and capacity of the FEA solution platform. However, specific to this study, considering the limitations mentioned above, it can be concluded that all FEA approaches developed to model the physical conditions for RDM were properly configured and suitable for use in structural analysis research.

### Conclusions

This study's objective was to conduct structural strength analysis using experimental and numerical methods that could be used in the structural design studies of a new tractor-mounted RDM and similar agricultural machineries. This paper covers the analyses for a specific RDM during harvesting. The mower was subjected to physical tests in the study that were compatible with structural strength analysis methods based on CAE. FEA simulations provided a useful visual output and numerical data for the machine's deformation behavior during harvesting. It can also be stated that a reasonable correlation was obtained between experimental and numerical results under pre-defined boundary conditions and limitations. Both experimental and simulation results revealed that there were no functional or structural failure indications on the structural components of the machine during harvesting. However, in order to complete the final design decisions which consider the machine's total work cycle, a related analysis should be conducted for the static linkage and transportation conditions of the machine. Thus, it may be possible to examine structural optimization indicators, the possibility of decreasing material weight and the overall cost of the machine, and other related topics. The study's main finding was the machine's structure specifically considered in this study works safely during harvesting conditions. Additionally, it can be stated that an effective FEA strategy could be significantly utilized in durability assessment and may reduce the amount of physical prototype testing, as well as production costs and lost time, during the design of agricultural machinery.

### References

- ANSYS Product Doc. 2019. ANSYS Meshing User's Guide: Skewness (Release 2019 R2). ANSYS Inc., USA. Available from: [https://ansyshelp.ansys.com/account/secured?returnurl=/Views/Secured/corp/v191/wb2\\_help/wb2\\_help.html](https://ansyshelp.ansys.com/account/secured?returnurl=/Views/Secured/corp/v191/wb2_help/wb2_help.html)
- Arac I. 2001. A research on comparison of different type mowers' performances (In Turkish). Yüzüncü Yıl University.
- Ariza O., Gilchrist S., Widmer R.P., Guy P., Ferguson S.J., Crompton P.A., Helgason B. 2015. Comparison of explicit finite element and mechanical simulation of the proximal femur during dynamic drop-tower testing. *J. Biomech.* 48:224-32.
- ASAE D497.7. 2011. Agricultural Machinery Management Data, 5. Available from: <https://elibrary.asabe.org/abstract.asp?aid=36431&t=2>
- Bi Z. 2021. Practical Guide to Digital Manufacturing. In *Practical Guide to Digital Manufacturing*. Springer Int. Pub. Available



- from: <https://doi.org/10.1007/978-3-030-70304-2>
- Bringas J.E. 2016. Handbook of Comparative World Steel Standards, 5th Edition. In J. E. Bringas (Ed.), Handbook of Comparative World Steel Standards, 5th Edition. ASTM Int. Available from: <https://doi.org/10.1520/ds67d-eb>
- Caliskan K. 2011. The optimisation of cab protective structure with finite element method simulation verified with laboratory tests (Ph.D. Thesis) (In Turkish). Ege University. Available from: [https://tez.yok.gov.tr/UlusalTezMerkezi/tezDetay.jsp?id=f\\_L98Wo9ne6PuW8451YkJA&no=X5TeCmrvjv3KhzPYC\\_XMB-IA](https://tez.yok.gov.tr/UlusalTezMerkezi/tezDetay.jsp?id=f_L98Wo9ne6PuW8451YkJA&no=X5TeCmrvjv3KhzPYC_XMB-IA)
- Cardarelli F. 2008. Materials Handbook: A Concise Desktop Reference. Materials Handbook (2nd ed.). London: Springer.
- Celik H.K., Akinci I. 2015. Analytical and Finite Element Method Based Stress Analysis of the Motion Transmission Axels of A Rotary Drum Mower (in Turkish). J. Agric. Mach. Sci. 11:247-55.
- Celik H.K., Akinci I. 2016. Analytical and Finite Element Method Based Stress Analysis of Rotary Elements: Case Study for the Motion Transmission Gears of a Rotary Drum Mower. J. Fail. Anal. Prev. 16:293-301.
- Celik H.K., Caglayan N., Çinar R., Ucar M., Ersoy H., Rennie A.E.W. 2012. Stress analysis of a sample marine crane's boom under static loading condition. Proceeding of 5th International Mechanical Engineering Forum 2012, June 20th-22nd, 246-55.
- Celik H.K., Caglayan N., Topakci M., Rennie A.E.W., Akinci I. 2020. Strength-based design analysis of a Para-Plow tillage tool. Comput. Electron. Agric. 169.
- Celik H.K., Rennie A.E.W., Akinci I. 2017. Design and structural optimisation of a tractor mounted telescopic boom crane. J. Braz. Soc. Mech. Sci. Eng. 39:909-24.
- Chakrabarty B.K. 2022. Integrated CAD by Optimization. In Integrated CAD by Optimization. Springer Int. Pub. Available from: <https://doi.org/10.1007/978-3-030-99306-1>
- Davis J.R. 1998. Metals Handbook. Asm Intl. 2571.
- Day B., Field L., Jarvis A. 2009. The Wrest Park Story 1924-2006 (Chapter 7 Post harvest processing). Biosyst. Eng. 103:79-89.
- Degirmencioglu A. 2003. Determination of Stress Under Load on a Three-Bottom Moulboard Plough Research Project: 98 ZRF046.
- El-Baily M.M. 2022. A study of rotary drum mower blade wear and its effects on forage productivity. Poljoprivredna Tehnika. 47:87-100.
- Eryürük Ş., Nesimioğlu B.I.S., Altun H.O., Açıkgöz H., Yumusak S., Yıldız H.B., Çalik A., Ethem Bağriyanik O.İ. 2019. Research and Development Approaches and Implementation Issues in Agricultural Machinery Sector; Konya Case. Procedia Comput. Sci. 158:235-43.
- HBM. 2011a. Datasheet: QuantumX MX840A. Doc. No: B2924-2.0 en (p. 16). Hottinger Baldwin Messtechnik GmbH. Available from: <https://www.sensor-hbm.com/upload/product-file/b2924.pdf>
- HBM. 2011b. Strain Gages and Accessories. Doc. No: S 1265-1.0 en (p. 100). Hottinger Baldwin Messtechnik GmbH. <http://www.hbm.ru/pic/pdf/1176378299.pdf>
- HBM Inc. 2022. DAQ Software, Data Acquisition Software, catman, HBM. Available from: [https://www.hbm.com/en/2290/catman-data-acquisition-software/?product\\_type\\_no=DAQ\\_Software](https://www.hbm.com/en/2290/catman-data-acquisition-software/?product_type_no=DAQ_Software)
- Hoffmann K. 1989. An Introduction to Measurements using Strain Gages. Hottinger Baldwin Messtechnik GmbH. Available from: [http://elektron.pol.lublin.pl/users/elekp/MNEQ\\_english/Hoffmann\\_An\\_Introduction\\_to\\_Measurements\\_using\\_Strain\\_Gages.pdf](http://elektron.pol.lublin.pl/users/elekp/MNEQ_english/Hoffmann_An_Introduction_to_Measurements_using_Strain_Gages.pdf)
- Horrocks R.D., Valentine J.F. 2000. Harvested Forages. 1st ed. Crop Sci. 40.
- Krutz G., Thompson L., Claar P. 1984. Design of agricultural machinery. In Design of Agric. Mach. John Wiley and Sons.
- Kulaksiz O. 1995. Tables in Metal Profession (Metal Mesleğinde Tablolar). Turkish Republic Ministry of National Education.
- Kuna M. 2013. Finite Elements in Fracture Mechanics. Springer Netherlands. 201.
- Kurowski P., Szabo B. 1997. How to find errors in finite-element models. Mach. Des. 1:93-8.
- Kutay G. 2003. The Machinist's Guide (1st ed.). Birsen Publication.
- Martinez-Valencia L., Camenzind D., Wigmosta M., Garcia-Perez M., Wolcott M. 2021. Biomass supply chain equipment for renewable fuels production: A review. Biomass Bioenergy. 148.
- Mesa J.A., Gonzalez-Quiroga A., Aguiar M.F., Jugend D. 2022. Linking product design and durability: A review and research agenda. Heliyon 8:e10734.
- MKE. 1978. MKE norm special steel types catalog (1st ed.). Machinery and Chemical Industry Corporation (MKE). Available from: [https://books.google.com.tr/books/about/MKE\\_normu\\_özel\\_nitelikte\\_Çelik\\_türler.html?id=g6DsxAEACAAJ&redir\\_esc=y](https://books.google.com.tr/books/about/MKE_normu_özel_nitelikte_Çelik_türler.html?id=g6DsxAEACAAJ&redir_esc=y)
- Paraforos D.S., Griepentrog H.W., Vougioukas S.G. 2016. Methodology for designing accelerated structural durability tests on agricultural machinery. Biosyst. Eng. 149:24-37.
- Rembold U., Nnaji B.O., Storr A. 1993. Computer Integrated Manufacturing and Engineering. J. Manuf. Syst. (1st ed.). Addison-Wesley Pub. Co.
- Rice R.C., Jackson J.L., Bakuckas J., Thompson S. 2003. Metallic Materials Properties Development and Standardization (MMPDS) (Issue January). U.S. Department of Transportation Federal Aviation Administration.
- Ruiz de Galarreta S., Jeffers J.R.T., Ghouse S. 2020. A validated finite element analysis procedure for porous structures. Mater. Des. 189:108546.
- Sabancı A., Akinci İ. 2012. Agricultural Tractors ( In Turkish) (1st ed.). Nobel Academic Publication.
- Srivastava A.K., Goering C.E., Rohrbach R.P., Buckmaster D.R. 2013. Engineering Principles of Agricultural Machines, Second Edition. Engineering Principles of Agricultural Machines, 2nd Edition.
- Theunissen P. 2002. An Economical Approach to Agricultural Machinery Management (1st ed.). Computus Management Information (Pty) Ltd.
- Torre R., Brischetto S. 2022. Experimental characterization and finite element validation of orthotropic 3D-printed polymeric parts. Int. J. Mech. Sci. 219:107095.
- TRMoFAL. 2001. Measurement of the Agricultural Values - Technical Instruction for Alfalfa Plant (Medicago L. species) (In Turkish). Turkish Republic, Ministry of Food, Agriculture and Livestock.
- TRMoNE. 2012. Fodder Plant Cultivation (Agricultural Technologies Lecture Notes) (In Turkish). TRMoNE: Turkish Republic Ministry of National Education. Available from: [http://megep.meb.gov.tr/mte\\_program\\_modul/moduller\\_pdf/BaklagilYemBitkileriYetistirciligi1.pdf](http://megep.meb.gov.tr/mte_program_modul/moduller_pdf/BaklagilYemBitkileriYetistirciligi1.pdf)
- Turker U. 1992. Determination of Cutting Resistance of Alfalfa plant (In Turkish). Akara University.
- Vishay. 2007. M-Bond 200 Adhesive - Material safety datasheet (MSDS#MGM007T/14027). Available from: <https://>

[louisville.edu/micronano/files/documents/safety-data-sheets-sds/m-bond-200-adhesive/](http://louisville.edu/micronano/files/documents/safety-data-sheets-sds/m-bond-200-adhesive/)

Walters R.D. 2021. Technical Note 21. Soil, Draft, and Traction Tillage Tool. Core AgriSystems. Agrosphere Int. Group. 1:1-9.  
Yuksel Tarim Inc. 2013. YUKSEL TARIM - Agricultural

Machinery Inc. Available from: <http://www.yukseltarim.com/>  
Yurdem H., Degirmencioglu A., Cakir E., Gulsoylu E. 2019. Measurement of strains induced on a three-bottom moldboard plough under load and comparisons with finite element simulations. Measurement. J. Int. Meas. Confed. 136:594-602.

Non-commercial use only